C–H Activation by [Bis(dialkoxyphosphino)ethane]platinum(0) and [Bis(diaminophosphino)ethane]platinum(0) Complexes: Platinum–Platinum Dimer Formation Limits Yields

Marjorie E. Squires, Dennis J. Sardella, and Lawrence B. Kool*

Department of Chemistry, Eugene Merkert Chemistry Center, Boston College, 2609 Beacon Street, Chestnut Hill, Massachusetts 02167-3860

Received December 28, 1993[⊗]

Syntheses of new bidentate phosphorus-containing ligands and platinacycles that insert into C–H bonds of unactivated hydrocarbons under mild conditions are reported. The reactivities of the platinum neopentyl hydride species can be substantially increased by introducing oxygen- or nitrogen-containing substituents onto the phosphorus atoms. Dimeric species that are formed from the Pt(0) species are identified by comparing their ^{31}P NMR spectra with simulated spectra. Further evidence for these dimers was obtained by cleaving them to mononuclear derivatives with alkyne and phosphine ligands. Formation of these dimers limits the efficiency of hydrocarbon activation. The extent of dimerization that occurs during alkane activation depends upon the steric crowdedness about the Pt(0) center. The X-ray structure of $[-(CH_2)_4-C(CH_2O)_2]PCH_2CH_2P[(OCH_2)_2C-(CH_2)_4-]Pt(neo\text{-}Pe)Cl$ (**9**) has been determined: $C_{21}H_{39}O_4PtCl_2{\cdot}CH_2Cl_2$, $M_r = 732.96$, monoclinic, space group $P2_1/n$ (No. 14), $a = 14.667(3)$ Å $b = 11.384(6)$ Å, $c = 17.110(4)$ Å, $\beta = 100.62(2)°$, $V = 2808(3)$ Å^3, $Z = 4$, $D_{calc} = 1.734$ g cm^{-3}, μ(Mo Kα) = 54.74 cm^{-1}, $R = 0.048$, $R_w = 0.055$.

The cleavage of unactivated C–H bonds of aliphatic hydrocarbons by addition to transition-metal atoms is now known to be an intrinsically facile process and occurs in many environments: on metal surfaces,[1] in organometallic compounds,[2–14] in the vapor phase,[15–19] or in inert matrices.[20] In 1988 Hackett and Whitesides[13,21] reported the activation of carbon–hydrogen bonds by the five-membered platinacycle $(Cy_2PCH_2CH_2PCy_2)Pt^0$ (Cy = cyclohexyl), a transient intermediate generated by the reductive elimination of neopentane from *cis*-hydridoneopentyl[bis(dicyclohexylphosphino)ethane]platinum(II). This work attracted attention because platinum and palladium are widely applied as components of heterogeneous catalysts used industrially on a large scale and have played prominent roles in recent studies of the functionalization of alkanes via C–H activation reactions.[22–26]

In this paper we report the syntheses of bidentate phosphorus-containing ligands and platinacycles derived from them that insert into C–H bonds of unactivated hydrocarbons under mild conditions. We have found that the reactivities of the platinum neopentyl hydride species can be increased substantially by introducing oxygen- or nitrogen-containing substituents onto the chelating phosphorus atoms. We also report the identification by ^{31}P NMR spectrometry of dimeric species that are formed during these C–H activation reactions. The formation of these dimers limits the yields of the hydrocarbon activation reactions. The varying tendencies of the different C–H activating fragments to dimerize can be understood by examining the degrees of steric congestion about the platinum atoms.

⊗ Abstract published in *Advance ACS Abstracts,* June 15, 1994.

(1) Ciapetta, E. G.; Wallace, D. N. *Catal. Rev.* **1971,** *5,* 67–158.
(2) Buchanan, J. M.; Stryker, J. M.; Bergman, R. G. *J. Am. Chem. Soc.* **1986,** *108,* 1537–1550.
(3) Bergman, R. G. *Science* **1984,** *223,* 902–908.
(4) Periana, R. A.; Bergman, R. G. *J. Am. Chem. Soc.* **1986,** *108,* 7332–7346.
(5) Field, L. D.; George, A. V.; Messerle, B. A. *J. Chem. Soc., Chem. Commun.* **1991,** *19,* 1339–1341.
(6) Jones, W. D.; Feher, F. J. *J. Am. Chem. Soc.* **1985,** *107,* 620–631.
(7) Ghosh, C. K.; Graham, W. A. G. *J. Am. Chem. Soc.* **1987,** *109,* 4726–4727.
(8) Crabtree, R. H. *Chem. Rev.* **1985,** *85,* 245–269.
(9) Jones, W. D.; Maguire, J. A. *Organometallics* **1987,** *6,* 1301–1311.
(10) Gretz, E.; Oliver, T. F.; Sen, A. *J. Am. Chem. Soc.* **1987,** *109,* 8109–8111.
(11) Ephritikhine, M. *Nouv. J. Chim.* **1986,** *10,* 9.
(12) Rothwell, I. P. *Polyhedron* **1985,** *4,* 177–200.
(13) Hackett, M.; Whitesides, G. M. *J. Am. Chem. Soc.* **1988,** *110,* 1449–1462.
(14) Periana, R. A.; Taube, D. J.; Evitt, E. R.; Löffler, D. G.; Wentrcek, G. V.; Masuda, T. *Science* **1993,** *259,* 340–343.
(15) Schilling, J. B.; Beauchamp, J. L. *J. Am. Chem. Soc.* **1988,** *110,* 15–24.
(16) Irikura, K. K.; Beauchamp, J. L. *J. Phys. Chem.* **1991,** *95,* 8344–8351.
(17) Ozin, G. A.; McIntosch, D. F.; Mitchell, S. A. *J. Am. Chem. Soc.* **1981,** *103,* 1574–1575.
(18) Billups, W. E.; Konarski, M. M.; Hange, R. H.; Margrave, J. L. *J. Am. Chem. Soc.* **1980,** *102,* 7393–7394.
(19) Klabunde, K. J.; Tanaka, Y. *J. Am. Chem. Soc.* **1983,** *105,* 3544–3546.
(20) Green, M. L. H.; O'Hare, D. *J. Chem. Soc., Chem. Commun.* **1985,** 355–356.
(21) Hackett, M.; Ibers, J. A.; Whitesides, G. M. *J. Am. Chem. Soc.* **1988,** *110,* 1436–1448.
(22) Stenberg, P. J.; Kool, L. B. The Catalytic Partial Oxidation of Methane by Platinum Black and Aqueous Ferric Sulfate, In *Structure of Jet Fuels III*; ACS Symposium Series; American Chemical Society: Washington, DC, 1992; pp 576–579.
(23) Shilov, A. E. *Activation of Saturated Hydrocarbons by Transition Metal Complexes;* D. Reidel: Dordrecht, The Netherlands, 1984.
(24) Hill, C. L., Ed. *Activation and Functionalization of Alkanes*; Wiley-Interscience: New York, 1989.
(25) Labinger, J. A.; Herring, A. M.; Bercaw, J. E. *J. Am. Chem. Soc.* **1990,** *112,* 5628–5629.
(26) Sen, A.; Lin, M. *J. Chem. Soc., Chem. Commun.* **1992,** 508–510.

0276-7333/94/2313-2970$04.50/0

Scheme 1. Syntheses of Bidentate Ligands 1–5

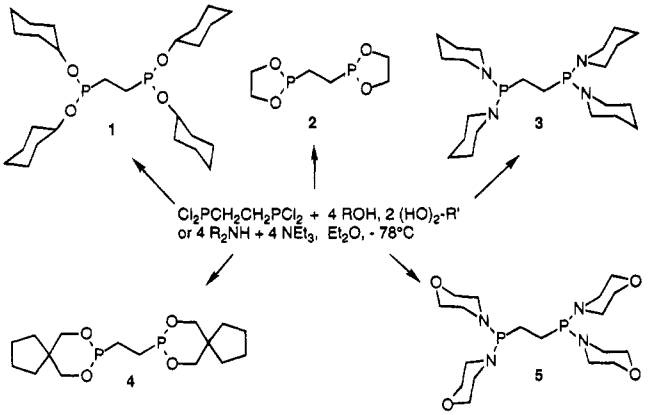

Results

Syntheses of Ligands. We obtained the bidentate ligands $(CyO)_2PCH_2CH_2P(OCy)_2$ (**1**; Cy = cyclohexyl), $(-OCH_2CH_2O-)PCH_2CH_2P(-OCH_2CH_2O-)$ (**2**), $(C_5H_{10}N)_2PCH_2CH_2P(NC_5H_{10})_2$ (**3**), $[-(CH_2)_4-C(CH_2O)_2]PCH_2CH_2P[(OCH_2)_2C-(CH_2)_4-]$ (**4**), and $(morph)_2PCH_2CH_2P(morph)_2$ (**5**) (morph = morpholino) in condensations at −78 °C of 1,2-bis(dichlorophosphino)ethane with mono- or difunctional alcohols or secondary amines in Et_2O (Scheme 1). This procedure provided materials that exhibited no extraneous signals in their ^{31}P NMR spectra. Compounds **1** and **2** were obtained as low-melting waxes, while **3–5** were waxy solids.

Syntheses of Platinum Complexes. Displacement of 1,5-cyclooctadiene from (1,5-cyclooctadiene)chloroneopentylplatinum(II)[27] in CH_2Cl_2 (Scheme 2) by ligands **1-5** and 2,2′-bipyridyl afforded the neopentyl chloride complexes $[(CyO)_2PCH_2CH_2P(OCy)_2]Pt(neo\text{-Pe})Cl$ (**6**; Np = *neo*-Pe, Cy = cyclohexyl), $[(C_5H_{10}N)_2PCH_2CH_2P(NC_5H_{10})_2]Pt(neo\text{-Pe})Cl$ (**7**), $[(morph)_2PCH_2CH_2P(morph)_2]Pt(neo\text{-Pe})Cl$ (**8**), $[-(CH_2)_4-C(CH_2O)_2]PCH_2CH_2P[(OCH_2)_2C-(CH_2)_4-]Pt(neo\text{-Pe})Cl$ (**9**), $[(-OCH_2CH_2O-)PCH_2CH_2P(-OCH_2CH_2O-)]Pt(neo\text{-Pe})Cl$ (**10**), and $(bpy)Pt(neo\text{-Pe})Cl$ (**11**) (bpy = 2,2′-bipyridyl) in excellent yields as air-stable, crystalline solids. Complexes **6–10** exhibited ^{31}P NMR spectra typical for five-membered platinacycles having bidentate phosphorus ligands[28] in which the two phosphorus atoms are inequivalent and appear as doublets (from P–P coupling) flanked by ^{195}Pt satellites. A comparison of the spectra of this series of neopentyl chlorides that have heteroatoms adjacent to phosphorus reveals that the phosphorus signals are shifted downfield with respect to complexes lacking these heteroatoms (cf. δ 65.0, 54.2 for $(Cy_2PCH_2CH_2PCy_2)Pt(neo\text{-Pe})Cl$ vs δ 176.4, 133.5 for $[(CyO)_2PCH_2CH_2P(OCy)_2]Pt(neo\text{-Pe})Cl$ (**6**)). This downfield shift presumably reflects a deshielding of the phosphorus atoms (and concomitant deshielding of the platinum atoms) attributable to back-bonding contributions from the phosphite portions of the ligands.[29] In addition, the platinum–phosphorus couplings observed for the complexes having heteroatoms are larger, reaching a maximum of 2162 and 6194 Hz for complex **9** (cf. 1611 and 4334 Hz for $(Cy_2PCH_2CH_2PCy_2)Pt(neo\text{-Pe})Cl$).

Scheme 2. Syntheses of Neopentyl Chloride Complexes 6–11

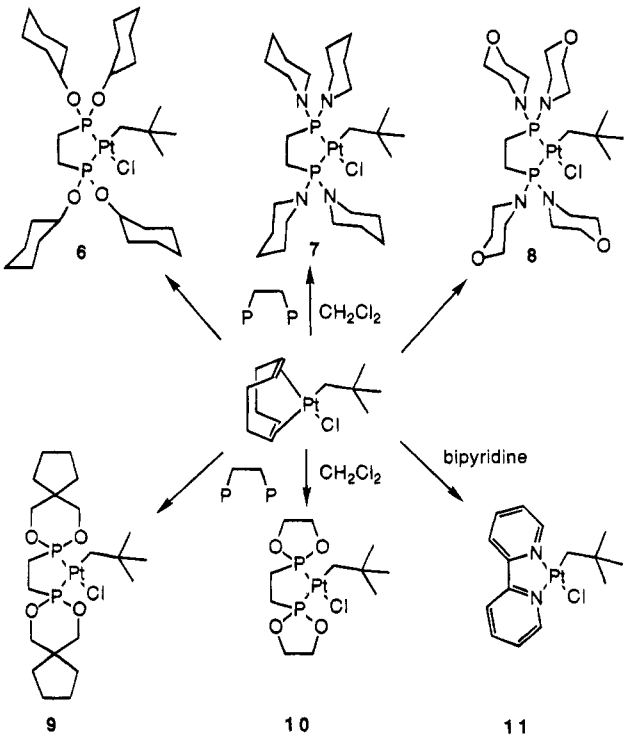

Scheme 3. Syntheses of Neopentyl Hydride Complexes 12–15

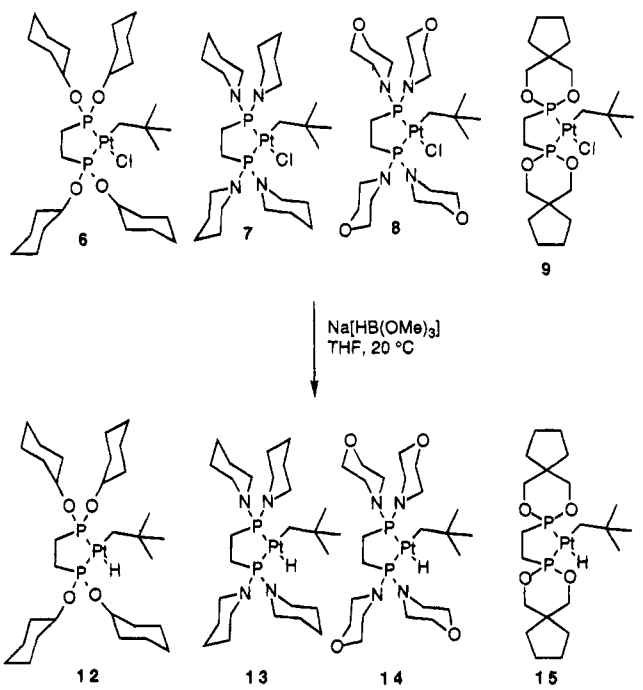

Reduction of the neopentyl chlorides **6–9** with $Na[HB(OMe)_3]$ in THF solution (Scheme 3), afforded the respective neopentyl hydrides **12–15** that were used in subsequent experiments in C–H activations. The progress of these reductions was followed by ^{31}P NMR spectroscopy of aliquots of the reacting mixtures. Complexes **12–15** were produced cleanly in these reductions within 5–10 min but exhibited limited stabilities toward

(27) Brainard, R. L.; Miller, T. M.; Whitesides, G. M. *Organometallics* **1986**, *5*, 1481–1490.
(28) Garrou, P. E. *Chem. Rev.* **1985**, *85*, 171–185.
(29) Collman, J. P.; Hegedus, L. S.; Norton, J. R.; Finke, R. G. *Principles and Applications of Organotransition Metal Chemistry*; University Science Books: Mill Valley, CA, 1987; pp 70–71.

reductive elimination, even at room temperature. This ease of conversion to neopentyl hydride contrasted markedly with the reaction times of 10–25 h reported for the conversion of $(Cy_2PCH_2CH_2PCy_2)Pt(neo\text{-}Pe)Cl$ to $(Cy_2PCH_2CH_2PCy_2)Pt(neo\text{-}Pe)H$ under the same conditions.[21] Similarly, the instabilities of complexes **12–15** toward reductive elimination at room temperature contrasted with the relative inertness of $(Cy_2PCH_2CH_2PCy_2)Pt(neo\text{-}Pe)H$, which was stable enough to allow structural determination by X-ray diffraction and required heating to 60 °C for reductive elimination to occur.[21] Our findings are in accord with a recent report by Roddick et al. which indicated that electron-withdrawing groups, i.e., chelating (perfluoroaryl)phosphine complexes, underwent reductive elimination much more readily than their non-perfluorinated analogues.[30] These findings also provide further corroboration of Hoffmann's theoretical proposition that reducing the electron-donor ability of the ancillary ligands should accelerate reductive elimination.[31]

Complex **10** could be reduced to neopentyl hydride but was insufficiently soluble in cyclohexane to permit ^{31}P NMR spectrometric analysis of any C–H activating reactivity. Treatment of the bipyridyl complex **11** with several different hydrides (sodium borohydride, lithium aluminum hydride, calcium hydride, etc.) even under mild conditions resulted in decomposition to black products.

C–H Activation Reactions. The reactivities of the neopentyl hydride complexes **12–15** toward C–H or C–D bonds of benzene, benzene-d_6, Me_4Si, and cyclohexane were compared by extracting freshly prepared samples into cyclohexane (the solvent determined to be least reactive in C–H activation experiments), adding the organic substrate, degassing in three freeze–pump–thaw cycles, and following the progress of the reactions by ^{31}P NMR spectrometry in sealed NMR tubes. Reductive elimination of neopentane from **12–15** generated coordinatively unsaturated platinacycles that inserted into C–H bonds of the substrates (eq 1). Activation

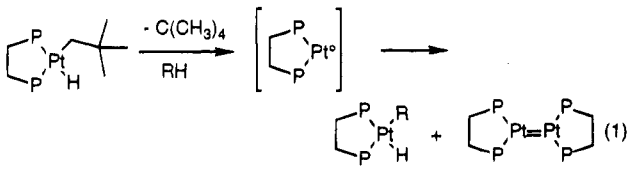

(1)

of cyclohexane was not observed in experiments with more reactive substrates such as benzene and TMS. In addition to products of oxidative addition from complexes **12–15**, signals attributable to dimeric species were also detected (*vide infra*). A typical ^{31}P NMR spectrum obtained during a reaction of neopentyl hydride **13** in a 1.0 M solution of TMS in cyclohexane is shown in Figure 1. The yields of the products of oxidative-addition reactions were determined by integration vs an internal standard (PPh_3) and are tabulated in Table 1.

These reactions were observed spectroscopically over a period of several hours, and in all cases signals assigned to three species were identified: neopentyl

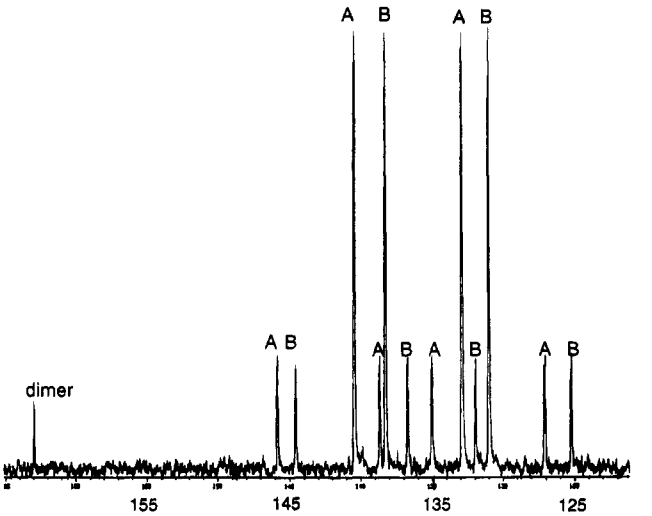

Figure 1. ^{31}P NMR spectrum obtained during the of reaction of neopentyl hydride **13** (signals A) with TMS in cyclohexane to form $[(C_5H_{10}N)_2PCH_2CH_2P(NC_5H_{10})_2]Pt(CH_2SiMe_2)H$ (signals B).

Table 1. Yields (%) of C–H Activation Reactions of Complexes 12-15

complex	C_6D_6[a]	C_6H_6[b]	C_6H_{12}[a]	$SiMe_4$[b]
12		94	4.3	77
13	75	48	39	100
14	85	insol	insol	insol

[a] Neat. [b] 1 M in cyclohexane.

hydride starting materials, alkyl or aryl hydride products of C–H activation, and a third species identified as Pt–Pt dimers, which were formed as side products at the expense of alkyl hydrides. In the case of complex **15**, and the six-membered platinacycle $(Cy_2PCH_2CH_2CH_2PCy_2)Pt(neo\text{-}Pe)H$ (**16**), analogous dimers were formed exclusively, without concomitant C–H activation. Signals assigned to a THF adduct, $(Cy_2PCH_2CH_2CH_2PCy_2)Pt(THF)$, were also detected momentarily at δ 23.16 (singlet with Pt satellites, J_{Pt-P} = 1891 Hz), before its eventual conversion to dimer (eq 2).

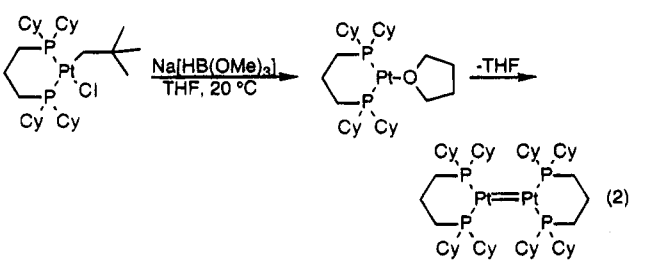

(2)

Spectroscopic Identification of the Dimeric Species. The ^{31}P NMR spectrum of the dimeric species formed from complex **15** is depicted in Figure 4, along with a simulated spectrum.[32] ^{195}Pt, the only magnetically active isotope of platinum, has a natural abundance of 33.7%. The combination of all other isotopes will be designated ^{19x}Pt. The dimeric species consists of a mixture of isotopomers, with the compositions and abundances listed in Table 2.

(30) Merwin, R. K.; Schnabel, R. C.; Koola, J. D.; Roddick, D. M. *Organometallics* **1992**, *11*, 2972–2978.
(31) Tatsumi, K.; Hoffmann, R.; Yamamoto, A.; Stille, J. K. *Bull. Chem. Soc. Jpn.* **1981**, *54*, 1857–1867.
(32) These simulations were obtained using VNMR software (Varian, Inc.) that includes an iterative spin simulation program based on the FORTRAN program LAME, also known as LAOCOON, with magnetic equivalence added. See: Bothner-by, A. A.; Castellani, S. *J. Chem. Phys.* **1964**, *41*, 3863.

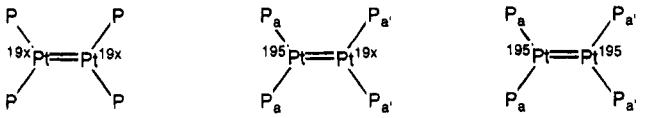

Figure 2. Three isotopomers in the mixture of dimers.

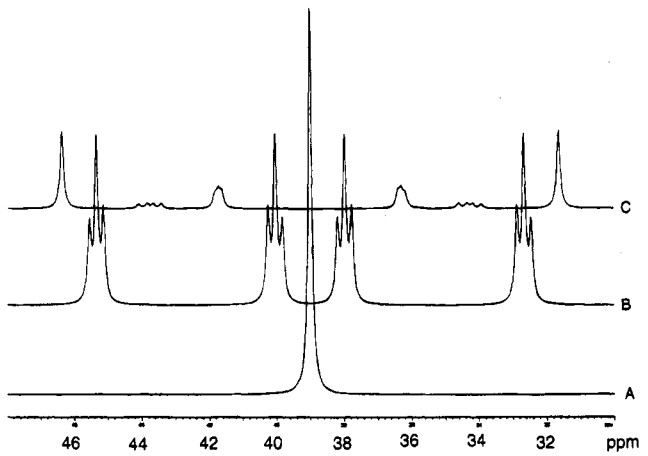

Figure 3. Simulated ^{31}P NMR spectra of (A) the [19*x*, 19*x*] dimer, (B) the [195, 19*x*] dimer, and (C) the [195, 195] dimer for $[(Cy_2PCH_2CH_2CH_2PCy_2)Pt]_2$.[33]

Table 2. Abundances (%) of Isotopomers in Dimer Mixture

composition	abundance	calculation
19*x*, 19*x*	44.0	0.663 × 0.663 × 100
195, 19*x*	44.7	0.663 × 0.337 × 2 × 100
195, 195	11.4	0.339 × 0.339 × 100

Each isotopomer (Figure 2) produces a unique ^{31}P NMR spectrum that depends on the presence or absence of Pt–P spin coupling and the magnetic equivalence or nonequivalence of the phosphorus atoms and the platinum atoms. In the first isotopomer, [19*x*, 19*x*], all four P atoms are equivalent and both Pt atoms are equivalent. This is expected to result in a single line in the ^{31}P spectrum (Figure 3, spectrum A).

The second isotopomer, [195, 19*x*], displays an $AX_2X'_2$ spectrum. The four phosphorus atoms are chemically equivalent (assuming a negligible Pt isotope effect on their chemical shifts) but magnetically nonequivalent: ^{195}Pt is coupled to P_a by a one-bond coupling (expected to be ca. 3000 Hz) and to $P_{a'}$ by a much smaller two-bond coupling. For the P_a atoms, the one-bond Pt–P coupling splits the P_a resonance into a doublet (spacing $^1J_{Pt-P}$). This produces an effective chemical shift difference of 0.5 [$^1J_{Pt-P}$] between the P_a and $P_{a'}$ phosphorus atoms, the coupling between them becomes visible, and each of the components of the doublet is split into a triplet (spacing $^3J_{P-P}$). For the $P_{a'}$ atoms, the two-bond Pt–P coupling splits the $P_{a'}$ resonance into a much smaller doublet (spacing $^2J_{Pt-P}$) than the one due to the P_a atoms. As before, this produces an effective chemical shift difference of 0.5 [$^2J_{Pt-P}$] between P_a and $P_{a'}$ phosphorus atoms, the coupling between them becomes visible, and each of the components of the doublet is split into a triplet (spacing $^3J_{P-P}$). The resultant spectrum of this isotopomer consists of two doublets of triplets located symetrically about the peak of the [19*x*, 19*x*] isotopomer (Figure 3, spectrum B). Thus, the magnitudes of $^1J_{Pt-P}$, $^2J_{Pt-P}$, and $^3J_{P-P}$ are directly measurable from the spectrum. The integrated intensities of the four triplets are identical. The fact that the geminal phosphorus atoms appear to be magnetically equivalent suggests D_{2d} symmetry for the molecule but is also consistent with a planar system of D_{2h} symmetry, in which rapid rotation about the Pt–Pt bond averages the cis and trans three-bond P–P couplings.

(33) The coupling constants used in this simulation were obtained from the actual spectrum and were $^1J_{Pt-P}$ = 2564.2 Hz, $^2J_{Pt-P}$ = 418.0 Hz, $^3J_{P-P}$ = 43.1 Hz, and $^1J_{Pt-Pt}$ = 1550 Hz. The line width at half height was found to be 25 Hz.

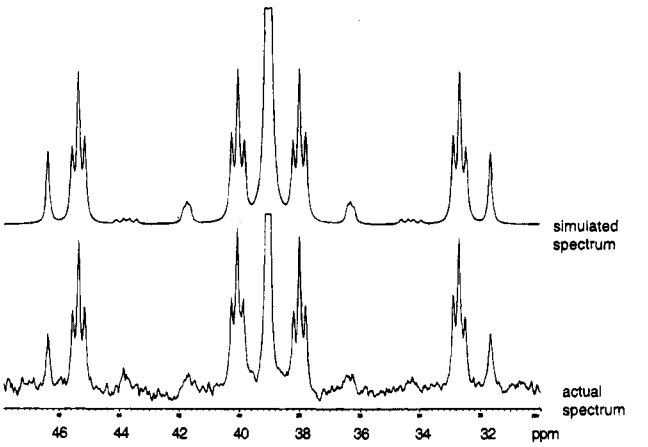

Figure 4. Simulated and actual ^{31}P NMR spectra for $[(Cy_2PCH_2CH_2CH_2PCy_2)Pt]_2$.

Table 3. Coupling Constants (Hz) for Pt–Pt Dimers from Simulated ^{31}P Spectra

complex	$^1J_{Pt-P}$	$^2J_{Pt-P}$	J_{P-P}	J_{Pt-Pt}
dimer from **12**	3163.5	496.8	71.00	1000 ± 50
dimer from **13**	2910.1	507.6	67.7	1200 ± 50
dimer from **14**	2895.4	479.6	72.4	1600 ± 50
dimer from **16**	2564.2	418.0	43.1	1550 ± 50

In the isotopomer with two magnetically active Pt atoms, [195, 195], the phosphorus atoms are again chemically equivalent but magnetically nonequivalent, because the couplings of P_a and $P_{a'}$ to a given platinum atom are still different. This leads to an $AX_2(AX_2)'$ spectrum. Since the two ^{195}Pt atoms are expected to be strongly coupled, with a symmetry-imposed chemical shift difference of 0, they act as a magnetic unit (virtual coupling). Thus, the spectrum of this isotopomer consists of an outer doublet symmetrically placed around the intense singlet, with a spacing $J_{AX} + J_{AX'}$ (Figure 3, spectrum C), along with four inner, less-intense, multiplets whose exact positions are dependent on the magnitude of $^1J_{Pt-Pt}$. Noniterative spectral simulations led to a value for $^1J_{Pt-Pt}$ of 1550 ± 50 Hz. The fact that the spacing of the outer doublet is larger than the sum of the one- and three-bond P–Pt couplings derived from the [195, 19*x*] isotopomer indicates that these couplings have the same sign. (No sign information for $^1J_{Pt-Pt}$ is available from the spectrum.)

The overall spectrum of the mixture of isotopomers is simply the weighted sum of these individual spectra, and the simulated and experimental spectra (Figure 4) are nearly identical.

The coupling constants derived in a similar manner for dimers formed from complexes **12**–**14** and **16** are given in Table 3.

The tendencies of complex **15** and the six-membered platinacycle $(Cy_2PCH_2CH_2CH_2PCy_2)Pt(neo\text{-}Pe)H$ (**16**) to dimerize upon reductive elimination reflect significant differences in the abilities of the substituents on the chelating ligands to shield the platinum atoms and

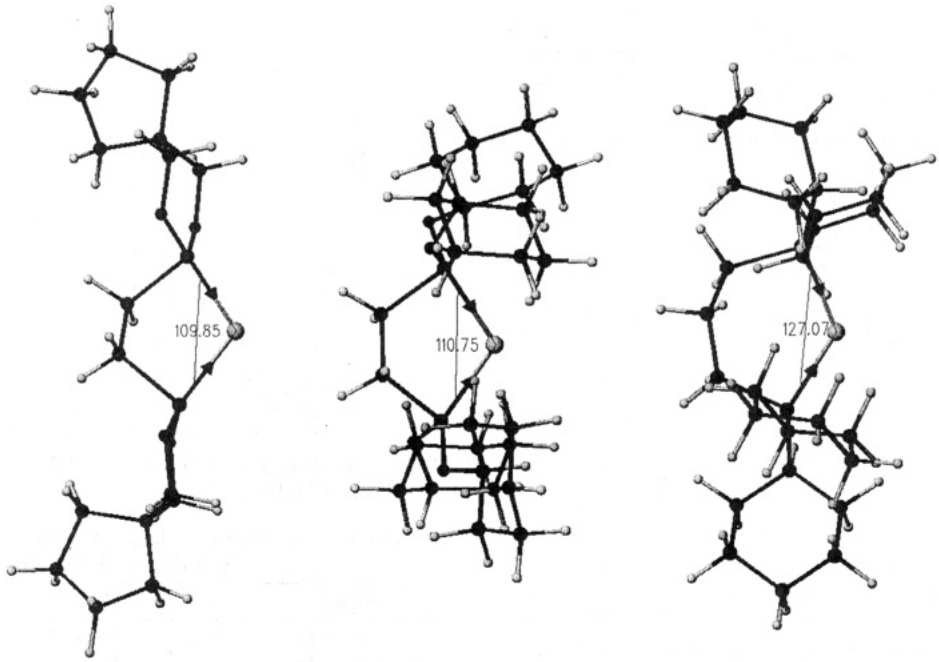

Figure 5. Comparison of minimized structures of $[-(CH_2)_4-C(CH_2O)_2]PCH_2CH_2P[(OCH_2)_2C-(CH_2)_4-]Pt$ (left) and $(Cy_2PCH_2CH_2CH_2PCy_2)Pt^0$ (right), which form dimers exclusively, and $(CyO)_2PCH_2CH_2P(OCy)_2Pt$ (center), which forms little dimer. The P−Pt−P angles are 109.8, 110.7, and 127.1°, respectively.

prevent the approach of a second metal fragment. This rationale is illustrated in Figure 5, in which structures of the three fragments $(CyO)_2PCH_2CH_2P(OCy)_2Pt^0$, $(Cy_2PCH_2CH_2CH_2PCy_2)Pt^0$, and $[-(CH_2)_4-C(CH_2O)_2]PCH_2CH_2P[(OCH_2)_2C-(CH_2)_4-]Pt^0$, minimized using an augmented version of MM2,[34] are compared.

^{31}P NMR signals assigned to these dimers gradually diminished over a period of up to 8 h at room temperature and persisted even longer when samples were stored at −20 °C. All our attempts to isolate and further characterize these dimeric species failed because of their eventual conversion to insoluble species. Neither FTIR nor ^1H NMR spectrometric measurements gave evidence of the presence of Pt−H bonds in these dimers. We attempted to activate benzene and other substrates by prolonged treatment with preformed dimers but obtained no evidence that the dimeric species inserted into C−H bonds. Treatment of dimer **17** with PhC≡CPh, MeC≡CMe, and PPh_3 did, however, result in rapid cleavage and the clean formation of the respective adducts **18**−**20** (eq 3). There is little precedent for

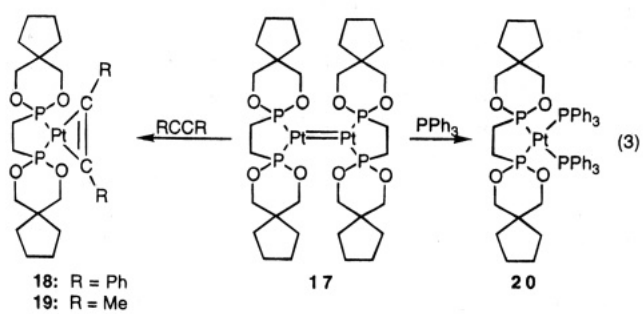

18: R = Ph
19: R = Me

17 **20**

complexes of the type Pt_2L_4. The complex $Pt_2(PPh_3)_4$, formed in the photolysis of $Pt_2(PPh_3)_4C_2O_4$, was reported in 1970 to be stable in air in the solid state.[35] No NMR spectra were reported. A dimeric platinum(0) complex, $[Pt(t\text{-}Bu)_2P(CH_2)_3P(t\text{-}Bu)_2]_2$, which is analogous to the dimer formed from **16**, has been reported previously.[36]

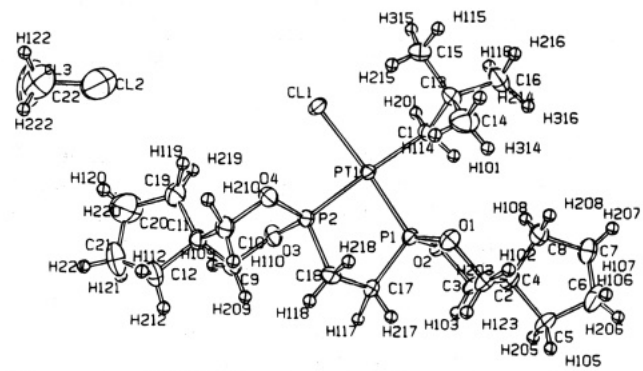

Figure 6. ORTEP drawing of **9**. Ellipsoids are drawn at the 50% probability level.

X-ray Crystal Structure of Complex 9. Because our rationalization of the differing abilities of these Pt(0) complexes to activate C−H bonds depends upon a reasonably accurate prediction of their structures, we undertook the determination of the X-ray crystal structure of complex **9** so that it could be compared with the models we had computed using molecular mechanics. Crystals suitable for X-ray structural determination were grown by slow concentration of solutions in CH_2Cl_2. The structure of complex **9** (Figure 6) consists of a distorted-square-planar platinum center with a P(1)−Pt−P(2) angle of 85.71° and a cis arrangement of the Cl and neopentyl groups. Selected interatomic distances and angles are given in Table 4, along with values obtained from our molecular mechanics calculations. The Pt−P(1) distance (2.167 Å) is 0.097 Å shorter than

(34) These structures were minimized using a CAChe Molecular Modeling System obtained from Tektronix, Inc. Augmented MM2 parameters were used, with a conjugate gradient with a relaxation factor of 1.00.

(35) Blake, D. M.; Nyman, C. J. *J. Am. Chem. Soc.* **1970**, *92*, 5359−5364.

(36) Yoshida, T.; Yamagata, T.; Tulip, T. H.; Ibers, J. A.; Otsuka, S. *J. Am. Chem. Soc.* **1978**, *100*, 2063−2073.

Table 4. Selected Interatomic Distances (Å) and Angles (deg) for Complex 9[a]

Pt–Cl	2.382(2) [2.292]	P(1)–O(2)	1.606(5) [1.597]
Pt–P(1)	2.167(2) [2.085]	P(1)–C(17)	1.812(7)
Pt–P(2)	2.264(2) [2.083]	Cl(1)–Pt–P(1)	172.79(7)
Pt–C(1)	2.116(7) [2.080]		
Cl(1)–Pt–P(2)	91.41(6) [93.11]	P(2)–Pt–C(1)	176.0(2)
Cl(1)–Pt–C(1)	92.2(2) [91.72]	Pt–P(1)–O(2)	114.3(2)
P(1)–Pt–P(2)	85.71(7) [80.17]	O(2)–P(1)–O(1)	104.5(3)
P(1)–Pt–C(1)	91.0(2) [95.05]		

[a] The values in brackets were obtained from molecular mechanics calculations.[37]

the Pt–P(2) distance (2.264 Å), which reflects the greater trans influence of the neopentyl group. The cyclopentyl groups of the bidentate ligand are sufficiently distant from the platinum center to preclude any intramolecular interaction between their C–H bonds and the platinum center of the Pt(0) species derived from **9**. Likewise, the oxygen atoms are constrained in their positions as members of six-membered rings to remain distant from direct interaction with the platinum atom. The presence of four spirocyclic centers results in a relatively rigid stucture with a sterically unencumbered platinum atom, and this rigidity is reflected in the tendency of **9** to form dimer **17** almost immediately after conversion to neopentyl hydride.

A comparison of the important bond distances and angles obtained crystallographically with those generated by molecular mechanics indicates they are in reasonable agreement. The largest errors in the calculated structure appear to arise from an underestimation of the Pt–P distances, which is also reflected in the P–Pt–P angle.

Conclusions

The introduction of oxygen and nitrogen substituents onto the phosphorus atoms of neopentyl hydrides of five-membered platinacycles results in more facile reductive elimination and activation of unactivated hydrocarbons. The yields of the resultant platinum alkyl hydrides are limited by the tendency of these Pt(0) fragments to dimerize. The extent of dimerization that occurs during alkane activation appears to depend upon the steric congestedness about the platinum(0) center. The dimers formed in these experiments were identified by ^{31}P NMR spectroscopy and compared with simulated spectra generated by the expected statistical mixture of isotopomers. Further evidence for the identities of the dimers was obtained by cleaving them to mononuclear derivatives having alkyne and phosphine ligands. Our future efforts will be aimed at strategies that minimize dimer formation.

Experimental Section

All operations were performed under a pure argon atmosphere using standard Schlenk techniques or in a Braun MB-150 drybox. THF and diethyl ether were purified by distillation under argon from sodium benzophenone. Cyclohexane, CH_2Cl_2, and triethylamine were purified by distillation from CaH_2. (1,5-Cyclooctadiene)platinum(II) chloride, 1,2-bis(dichlorophosphino)ethane, cyclohexanol, dicyclohexylamine, piperidine, morpholine, bipyridyl, sodium trimethoxyborohydride, 1,4-dibromobutane, 1,3-propanediol, tetramethylsilane, and 1-bromo-2,2-dimethylpropane were used as received from Aldrich Chemical Co. without purification. NMR spectra were obtained on Bruker AM 300, Varian XL300, or Varian Unity 500 spectrometers. ^{31}P NMR spectra were run at either 121.42 or 202.3 MHz. Chemical shifts are reported in ppm relative to residual solvent protons. ^{31}P shifts are reported in ppm relative to an internal PPh_3 standard at δ −4.70 obtained vs an internal H_3PO_4 reference at δ 0, with shifts downfield considered positive. A 90° pulse and a relaxation delay of at least $5T_1$ were used to ensure accurate quantitative integration. IR spectra were recorded on a Nicolet 510 spectrophotometer. 1,1-Bis(carboxyethyl)cyclopentane,[38] (1,5-cyclooctadiene)dineopentylplatinum(II),[39] and chloro(1,5-cyclooctadiene)neopentylplatinum(II) were prepared by published methods. The Grignard reagent was prepared from 1-bromo-2,2-dimethylpropane and magnesium turnings in THF. It was titrated with 2-butanol/toluene under argon with napth-1-ylphenylamine[40] as an indicator. Bidentate ligands of type $(RO)_2PCH_2CH_2P(OR)_2$ were prepared using procedures analogous to those reported for $(CH_3O)_2PCH_2CH_2P(OCH_3)_2$.[41]

$(CyO)_2PCH_2CH_2P(OCy)_2$ (1). A solution of NEt_3 (8.4 mL, 60 mmol, 4 equiv) and cyclohexanol (6.2 mL, 60 mmol, 4 equiv) in Et_2O (300 mL) in a Schlenk flask equipped with an efficient magnetic stirring bar or an overhead shaft stirrer and a pressure-equalizing addition funnel was treated dropwise over 30 min at −78 °C with 1,2-bis(dichlorophosphino)ethane (2.45 mL, 15 mmol) dissolved in 20 mL of Et_2O. During the addition triethylamine hydrochloride precipitated as a thick, white solid, making magnetic stirring difficult. After it was gradually warmed to room temperature overnight, the mixture was filtered through a Schlenk frit with liberal washing with Et_2O. The solvent was removed *in vacuo*, and $(CyO)_2PCH_2CH_2P(OCy)_2$ was obtained as a white wax (6.56 g, 90%). Mp: <20 °C. ^{31}P NMR (25 °C, $CDCl_3$): δ 173. ^{1}H NMR (25 °C, $CDCl_3$): δ 2.0–1.5 (m), 4.32 (s), 3.3–4.2 (m). ^{13}C NMR ($CDCl_3$, 20 °C): δ 25.5, 29.0, 36.4, 77.5. IR (KBr, cm^{-1}): 3439 (m), 2913 (vs), 2859 (vs), 2664 (w), 2361 (m), 1729 (m), 1659 (w), 1450 (vs), 1411 (m), 1372 (m), 1269 (vs), 1073 (vs), 927 (s), 891 (s), 877 (s), 845 (s), 809 (m), 788 (m).

$(-OCH_2CH_2O-)PCH_2CH_2P(-OCH_2CH_2O-)$ (2). In a similar manner, 1,2-ethanediol (2.04 g, 17.2 mmol), NEt_3 (4.8 mL, 35 mmol), and 1,2-bis(dichlorophosphino)ethane (2.0 g, 8.6 mmol) afforded $(-OCH_2CH_2O-)PCH_2CH_2P(-OCH_2CH_2O-)$ as a white wax that could be purified by recrystallization at low temperature from Et_2O (2.4 g, 87%). Mp: <20 °C. ^{31}P NMR (25 °C, $CDCl_3$): δ 40.5. ^{1}H NMR (25 °C, $CDCl_3$): δ 1.31 (d, 8 H, J_{PH} = 10 Hz), 2.05 (m, 4 H, PCH_2).

$(C_5H_{10}N)_2PCH_2CH_2P(NC_5H_{10})_2$ (3). Triethylamine (4.8 mL, 34.4 mmol), piperidine (3.4 mL, 34 mmol), and 1,2-bis(dichlorophosphino)ethane (2.0 g, 8.6 mmol) afforded $(C_5H_{10}N)_2PCH_2CH_2P(NC_5H_{10})_2$ as a white waxy solid (3.48 g, 95%). Mp: 125–127 °C. ^{31}P NMR (25 °C, $CDCl_3$): δ 89.5. ^{1}H NMR (25 °C, $CDCl_3$): δ 2.8–3.1 (m), 1.3–1.7 (m). IR (KBr, cm^{-1}): 2931, 2846, 2827, 2805, 2727, 2664, 2544, 2298, 1631, 1447, 1441, 1423, 1401, 1370, 1350, 1322, 1307, 1272, 1258, 1209, 1153, 1117, 1048, 1068, 1029, 927, 850, 829, 807, 724, 701, 534, 522, 681.

$[-(CH_2)_4-C(CH_2O)_2]PCH_2CH_2P[(OCH_2)_2C-(CH_2)_4-]$ (4). 1,1-Bis(carboxyethyl)cyclopentane[38] (0.81 g, 6.22 mmol), NEt_3 (1.9 mL, 14 mmol), and bis(dichlorophosphino)ethane (0.47 mL, 3.1 mmol) afforded $[-(CH_2)_4-C(CH_2O)_2]PCH_2CH_2P[C(CH_2O)_2-$

(37) The values obtained from these molecular mechanics calculations are included in order to provide an accurate sense of the level of approximation that can be expected when molecular mechanics methods are used to model these types of complexes. Molecular mechanics calculations do not include electronic factors such as the trans effect but are nevertheless useful in providing models to be used to assess gross steric differences in a series of closely related complexes.

(38) Vogel, A. I. *J. Chem. Soc.* **1929**, 1487–1494.
(39) Foley, P.; DiCosimo, R.; Whitesides, G. M. *J. Am. Chem. Soc.* **1980**, *102*, 6713–6725.
(40) Watson, S. C.; Eastham, J. F. *J. Organomet. Chem.* **1967**, *9*, 465–469.
(41) King, R. B.; Rhee, W. M. *Inorg. Chem.* **1978**, *17*, 2961–2963.

$(CH_2)_4-$] as a white, crystalline solid in quantitative yield (1.1 g). Mp: 79–81 °C. ^{31}P NMR (25 °C, $CDCl_3$): δ 163.8. ^1H NMR (25 °C, $CDCl_3$): δ 3.94 (m, 4H, PCH_2), 3.55 (s, 8 H, OCH_2), 1.57, 1.39 (m, 16 H, ring CH_2).

(morph)$_2$PCH$_2$CH$_2$P(morph)$_2$ (5). Using a similar procedure, triethylamine (1.3 mL, 17 mmol), morpholine (1.5 mL, 17 mmol), and 1,2-bis(dichlorophosphino)ethane (1.0 g, 4.3 mmol) afforded (morph)$_2$PCH$_2$CH$_2$P(morph)$_2$ as a white solid (1.5 mg, 80%). Mp: 107 °C. ^{31}P NMR (25 °C, $CDCl_3$): δ 88.4. ^1H NMR (25 °C, $CDCl_3$): δ 2.10–1.92 (m, 8 H, $-OCH_2$), 1.54–1.38 (m, 8 H, NCH_2), 0.11 (vt, 4 H, J_{PH} = 5 Hz). ^{13}C NMR (25 °C, $CDCl_3$): δ 69.4, 50.8, 45.5. IR (KBr, cm^{-1}): 2973–2818 (br, s), 1954 (m), 1645 (br, m), 1448 (s), 1363 (s), 1300 (s), 1258 (s), 1166 (s), 1110 (s), 1068, 1008 (s), 934 (br, s), 842 (m), 695 (br, s), 582 (m), 477.

[(CyO)$_2$PCH$_2$CH$_2$P(OCy)$_2$]Pt(*neo*-Pe)Cl (6). A Schlenk tube was charged with (CyO)$_2$PCH$_2$CH$_2$P(OCy)$_2$ (**1**; 415 mg, 0.853 mmol) dissolved in 25 mL of CH_2Cl_2. (1,5-Cyclooctadiene)chloroneopentylplatinum(II) (350 mg, 0.85 mmol) was gradually added under argon with stirring. A light yellow solution formed. After overnight stirring the solvent was removed *in vacuo*, the residue was dissolved in Et_2O, and the solution was filtered through a Schlenk frit. Concentration and cooling resulted in the formation of white crystals of [(CyO)$_2$PCH$_2$CH$_2$P(OCy)$_2$]Pt(*neo*-Pe)Cl (60%). Mp: 144–145 °C. ^{31}P NMR (25 °C, C_6D_6): δ 175 (d with Pt satellites, J_{P-P} = 12 Hz, J_{Pt-P} = 2014 Hz), 130 (d with Pt satellites, J_{P-P} = 12 Hz, J_{Pt-P} = 5785 Hz). ^1H NMR (25 °C, $CDCl_3$): δ 2.0–2.3 (m), 1.1–1.9 (m). Anal. Calcd for $C_{31}H_{59}ClO_4P_2Pt$: C, 47.23; H, 7.54. Found: C, 47.29; H, 7.70. IR (KBr, cm^{-1}): 2930, 2860, 2660, 1470, 1450, 1410, 1370, 1250, 1230, 1190, 1150, 1030, 980, 890, 880, 860, 820, 790, 730, 680, 550, 510, 500, 460, 400, 300.

[(C$_5$H$_{10}$N)$_2$PCH$_2$CH$_2$P(NC$_5$H$_{10}$)$_2$]Pt(*neo*-Pe)Cl (7). A solution was prepared containing (C$_5$H$_{10}$N)$_2$PCH$_2$CH$_2$P(NC$_5$H$_{10}$)$_2$ (**3**; 214 mg, 0.503 mmol) and (1,5-cyclooctadiene)chloroneopentylplatinum(II) (206 mg, 0.503 mmol) in 10 mL of CH_2Cl_2 in a Schlenk tube. After the mixture was stirred overnight at room temperature, the solvent was evaporated to deposit [(C$_5$H$_{10}$N)$_2$PCH$_2$CH$_2$P(NC$_5$H$_{10}$)$_2$]Pt(*neo*-Pe)Cl as a crystalline white solid (99%). Mp: 147–153 °C dec. ^{31}P NMR (25 °C, THF): δ 113.2 (s with Pt satellites, J_{Pt-P} = 2005 Hz), 88.3 (s with Pt satellites, J_{Pt-P} = 5264 Hz). ^1H NMR (25 °C, $CDCl_3$): δ 1.0 (s), 1.4–1.6 (m), 2.85–3.1 (m), 3.1–3.25 (m). Anal. Calcd for $C_{27}H_{55}ClN_4P_2Pt$: C, 44.53; H, 7.61; N, 7.69. Found: C, 44.73; H, 7.44; N, 6.71. IR (KBr, cm^{-1}): 2938 (s), 2846 (s), 1447 (w), 1405 (w), 1370 (w), 1257 (w), 1208 (m), 1152 (m), 1117 (m), 1053 (s), 1025 (w), 941 (s), 821 (m), 695 (m), 554 (w), 533 (m), 450 (w).

[(morph)$_2$PCH$_2$CH$_2$P(morph)$_2$]Pt(*neo*-Pe)Cl (8). By a similar method, (1,5-cyclooctadiene)chloroneopentylplatinum(II) (500 mg, 1.22 mmol) and (morph)$_2$PCH$_2$CH$_2$P(morph)$_2$ (**5**; 540 mg, 1.22 mmol) in 20 mL of CH_2Cl_2 afforded **8** as a white crystalline solid. Mp: 208–210 °C dec. ^{31}P NMR (25 °C, THF): δ 120.9 (s with Pt satellites, J_{Pt-P} = 1996 Hz), 100.6 (s with Pt satellites, J_{Pt-P} = 5256 Hz). ^1H NMR (25 °C, $CDCl_3$): δ 0.047 (s, 4 H, CH_2), 1.08 (s, 9 H, CH_3), 1.4–2.0 (m, 2 H, CH_2), 3.3 (d, 12 H, CH_2), 3.6 (d, 12 H, CH_2). Anal. Calcd for $C_{23}H_{47}ClN_4O_4P_2Pt$: C, 37.53; H, 6.44; N, 7.61. Found: C, 37.26; H, 6.41; N, 7.22. IR (KBr, cm^{-1}): 3430 (w), 3135 (w), 2952 (w), 2889 (vw), 2853 (w), 1637 (vw), 1459 (w), 1398, 1293 (vw), 1257, 1110 (s), 1075, 1018 (vw), 955 (s), 913 (w), 842 (vw), 821 (vw), 702 (w), 491 (w).

[$-$(CH$_2$)$_4-$C(CH$_2$O)$_2$]PCH$_2$CH$_2$P[(OCH$_2$)$_2$C$-$(CH$_2$)$_4-$]Pt(*neo*-Pe)Cl (9). A solution of [$-$(CH$_2$)$_4-$C(CH$_2$O)$_2$]PCH$_2$CH$_2$P[(OCH$_2$)$_2$C$-$(CH$_2$)$_4-$] (**4**; 691 mg, 2.00 mmol) and (1,5-cyclooctadiene)chloroneopentylplatinum(II) (820 mg, 2.0 mmol) in 20 mL of CH_2Cl_2 was stirred at room temperature. An immediate, exothermic reaction occurred in which the solution warmed to reflux temperature for ca. 1 min. After overnight stirring the solution was concentrated and cooled until white crystals of **9** formed (93%). ^{31}P NMR (25 °C, $CDCl_3$): δ 183 (d with Pt satellites, J_{P-P} = 7 Hz, J_{Pt-P} = 2162 Hz), 133 (d with Pt satellites, J_{P-P} = 7 Hz, J_{Pt-P} = 6194 Hz). ^1H NMR (25 °C, $CDCl_3$): δ 1.1 (s), 1.5–1.9 (m). Anal. Calcd for $C_{21}H_{39}O_4P_2PtCl$: C, 38.92; H, 6.07. Found: C, 38.65; H, 5.94. IR (KBr, cm^{-1}): 3429 (s), 2951 (vs), 2868 (vs), 2369 (vw), 1722 (vw), 1659 (vw), 1455 (w), 1413 (w), 1259 (s0, 1102 (vs), 1033 (s), 1013 (s), 965 (s), 822.

[($-$OCH$_2$CH$_2$O$-$)PCH$_2$CH$_2$P($-$OCH$_2$CH$_2$O$-$)]Pt(*neo*-Pe)Cl (10). The same procedure with (1,5-cyclooctadiene)chloroneopentylplatinum(II) (717 mg, 1.75 mmol) and ($-$OCH$_2$CH$_2$O$-$)PCH$_2$CH$_2$P($-$OCH$_2$CH$_2$O$-$) (**2**; 418 mg, 1.75 mmol) in 10 mL of CH_2Cl_2 yielded **10** (95%). ^{31}P NMR (25 °C, $CDCl_3$): δ 187 (s with Pt satellites, J_{Pt-P} = 2100 Hz), 158 (s with Pt satellites, J_{Pt-P} = 5990 Hz).

(bpy)Pt(*neo*-Pe)Cl (11). A procedure similar to that reported for (bpy)Pt(Me)Cl[42] was followed. (1,5-Cyclooctadiene)chloroneopentylplatinum(II) (175 mg, 0.427 mmol) in 5 mL of CH_2Cl_2 was treated with 2,2′-bipyridine (167 mg, 0.64 mmol). The solution was heated to reflux temperature for 3 h, during which time it turned canary yellow. The solution was then concentrated, and a few drops of diethyl ether were added. When this mixture was cooled to 0 °C, yellow crystals of **11** were obtained (185 mg, 95%) that contained 1 equiv of CH_2Cl_2. Mp: 217 °C dec. ^1H NMR (25 °C, $CDCl_3$): δ 1.11 (s, 9 H, *neo*-Pe), 2.17 (t, 2 H, CH_2, J_{Pt-H} = 44 Hz), 7.55, 8.0 (m, 8 H, bpy). Anal. Calcd for $C_{16}H_{21}Cl_3N_2Pt$: C, 35.40; H, 3.90; N, 5.16. Found: C, 36.30; H, 3.89; N, 4.86. IR (KBr, cm^{-1}): 3806, 2960 (s), 2894 (w), 2853 (s), 2804 (w), 1600 (s), 1466 (vs), 1447 (vs), 1380 (w), 1358 (w), 1311 (w), 1262 (w), 1158, 1144, 1104, 1068, 1020, 804, 760 (vs), 735, 642 (w).

[(CyO)$_2$PCH$_2$CH$_2$P(OCy)$_2$]Pt(*neo*-Pe)H (12). A solution of [(CyO)$_2$PCH$_2$CH$_2$P(OCy)$_2$]Pt(*neo*-Pe)Cl (**6**) (200 mg, 0.25 mmol) in 20 mL of THF was treated dropwise with a solution of Na[HB(OMe)$_3$] (100 mg, 0.78 mmol) in ca. 5 mL of THF at 20 °C. Cloudiness developed in a few minutes. The reaction was followed by ^{31}P NMR spectrometry, which indicated the reaction was complete in 0.5 h. The solvent was removed *in vacuo*, the residue was extracted with diethyl ether, and the solution was filtered. Concentration and cooling failed to provide a crystalline product. Concentrated solutions darkened even when maintained at −20 °C. Attempts to crystallize the complex from ether/hexane, cyclopentane, and cyclohexane were similarly unsuccessful. Complete removal of the solvent deposited an off-white solid that turned pink (reversibly) under high vacuum. ^{31}P NMR (25 °C, THF): δ 194 (d with Pt satellites, J_{P-P} = 38 Hz, J_{Pt-P} = 2314 Hz), 185.2 (d with Pt satellites, J_{P-P} = 38 Hz, J_{Pt-P} = 2558 Hz). IR (KBr, cm^{-1}): 2010 (w, Pt—H).

[(CyO)$_2$PCH$_2$CH$_2$P(OCy)$_2$]Pt(C$_6$H$_5$)H. A solution of [(CyO)$_2$PCH$_2$CH$_2$P(OCy)$_2$]Pt(*neo*-Pe)H (**12**) in 1.0 M benzene in cyclohexane was placed in an NMR tube and subjected to three freeze–pump–thaw cycles. The NMR tube was sealed, while frozen, under vacuum, and the reaction was followed by ^{31}P NMR spectrometry. Within 30 min at 30 °C the hydride was converted to an orange solution of [(CyO)$_2$PCH$_2$CH$_2$P(OCy)$_2$]Pt(C$_6$H$_5$)H (94%). ^{31}P NMR (25 °C, C_6D_6): δ 192.0 (d with Pt satellites, J_{P-P} = 38 Hz, J_{Pt-P} = 2413 Hz), 181.8 (d with Pt satellites, J_{P-P} = 38 Hz, J_{Pt-P} = 2450 Hz).

[(CyO)$_2$PCH$_2$CH$_2$P(OCy)$_2$]Pt(C$_6$D$_5$)D. A solution of [(CyO)$_2$PCH$_2$CH$_2$P(OCy)$_2$]Pt(*neo*-Pe)H (**12**) in C_6D_6 was placed in an NMR tube and subjected to three freeze–pump–thaw cycles. The NMR tube was sealed, while frozen, under vacuum and the reaction was followed by ^{31}P NMR spectrometry. Within 30 min at 60 °C the hydride was converted to an orange solution of [(CyO)$_2$PCH$_2$CH$_2$P(OCy)$_2$]Pt(C$_6$D$_5$)D (99%). ^{31}P NMR (25 °C, C_6D_6): δ 190.9 (d with Pt satellites, J_{P-P} = 36 Hz, J_{Pt-P} = 2412 Hz), 180.7 (t of d, J_{P-D} = 37 Hz, J_{P-P} = 37 Hz, J_{Pt-P} = 2464 Hz).

[(CyO)$_2$PCH$_2$CH$_2$P(OCy)$_2$]Pt(C$_6$H$_{11}$)H. A freshly prepared sample of [(CyO)$_2$PCH$_2$CH$_2$P(OCy)$_2$]Pt(*neo*-Pe)H (**12**)

(42) Clark, H. C.; Manzer, L. E. *J. Organomet. Chem.* **1973**, *59*, 411–428.

was dissolved in cyclohexane (saturated at room temperature) and transferred to an NMR tube. The tube was then subjected to three freeze–pump–thaw cycles to remove dissolved gases and sealed under vacuum while frozen. The reaction was followed by ^{31}P NMR at 35 °C. This procedure produced the cyclohexyl hydride in 4.3% yield. ^{31}P NMR (25 °C, cyclohexane): δ 192.5 (d with Pt satellites unresolved, J_{P-P} = 31 Hz), 182.2 (d with Pt satellites unresolved, J_{P-P} = 39 Hz).

[(CyO)$_2$PCH$_2$CH$_2$P(OCy)$_2$]Pt(CH$_2$SiMe$_2$)H. A saturated solution of [(CyO)$_2$PCH$_2$CH$_2$P(OCy)$_2$]Pt(*neo*-Pe)H (**12**) in 1.0 M TMS in cyclohexane was sealed in an NMR tube after three freeze–pump–thaw cycles. Heating to 30 °C for a few minutes produced signals corresponding to the C–H activated product in 74% yield. ^{31}P NMR (25 °C, cyclohexane): δ 190.3 (d with Pt satellites, J_{P-P} = 36 Hz, J_{Pt-P} = 2667 Hz), 185.3 (d with Pt satellites, J_{P-P} = 37 Hz, J_{Pt-P} = 2482 Hz).

{[(CyO)$_2$PCH$_2$CH$_2$P(OCy)$_2$]Pt}$_2$. Upon standing, solutions of the neopentyl hydride **12** in cyclohexane exhibited signals assigned to this dimeric species. ^{31}P NMR (25 °C, cyclohexane): δ 219.2 (J_{Pt-P} = 467, 3180, 3628 Hz).

[(C$_5$H$_{10}$N)$_2$PCH$_2$CH$_2$P(NC$_5$H$_{10}$)$_2$]Pt(*neo*-Pe)H (13). A procedure analogous to that given above for **12** was followed, in which [(C$_5$H$_{10}$N)$_2$PCH$_2$CH$_2$P(NC$_5$H$_{10}$)$_2$]Pt(*neo*-Pe)Cl (**7**) was treated with Na[HB(OMe)$_3$] in THF. ^1H NMR (THF-d_8, 20 °C): δ 3.43 (s, 8 H), 2.56 (s, 8H), 2.05 (t, 2H with Pt satellites, J_{Pt-H} = 153.9 Hz, J_{P-H} = 7.8 Hz), 1.5–1.8 (m, 28 H), –1.37 (d, 1H, with Pt satellites, J_{P1-H} = 224 Hz, J_{P2-H} = 13 Hz, J_{Pt-H} = 1132 Hz), –1.82 (d, 1H, with Pt satellites, J_{P1-H} = 224 Hz, J_{P2-H} = 13 Hz, J_{Pt-H} = 1133 Hz). ^{31}P NMR (25 °C, cyclohexane): δ 139.7 (d with Pt satellites, J_{P-P} = 11 Hz, J_{Pt-P} = 2233 Hz), 132.0 (d with Pt satellites, J_{P-P} = 11 Hz, J_{Pt-P} = 2387 Hz).

[(C$_5$H$_{10}$N)$_2$PCH$_2$CH$_2$P(NC$_5$H$_{10}$)$_2$]Pt(C$_6$D$_5$)D. A solution of [(C$_5$H$_{10}$N)$_2$PCH$_2$CH$_2$P(NC$_5$H$_{10}$)$_2$]Pt(*neo*-Pe)H (**13**) in C$_6$D$_6$ was placed in an NMR tube and subjected to three freeze–pump–thaw cycles. The mixture was heated at 50 °C for *ca.* 10 h. The reaction was followed by ^{31}P NMR spectrometry in a sealed tube. This produced [(C$_5$H$_{10}$N)$_2$PCH$_2$CH$_2$P(NC$_5$H$_{10}$)$_2$]Pt(C$_6$D$_5$)D in 75% yield. ^{31}P NMR (25 °C, C$_6$D$_6$): δ 133.8 (d with Pt satellites, J_{P-P} = 7 Hz, J_{Pt-P} = 2318 Hz), 127.2 (t of d, with Pt satellites, J_{P-P} = 7 Hz, J_{P-D} = 33 Hz, J_{Pt-P} = 2293 Hz).

[(C$_5$H$_{10}$N)$_2$PCH$_2$CH$_2$P(NC$_5$H$_{10}$)$_2$]Pt(C$_6$H$_5$)H. A solution of [(C$_5$H$_{10}$N)$_2$PCH$_2$CH$_2$P(NC$_5$H$_{10}$)$_2$]Pt(*neo*-Pe)H (**13**) in 1.0 M C$_6$H$_6$ in cyclohexane was placed in an NMR tube and degassed by means of three freeze–pump–thaw cycles. The reaction was followed by ^{31}P NMR spectrometry while the reaction mixture was gradually heated from 25 to 50 °C in a sealed tube. This produced [(C$_5$H$_{10}$N)$_2$PCH$_2$CH$_2$P(NC$_5$H$_{10}$)$_2$]Pt(C$_6$H$_5$)H in 48% yield. ^{31}P NMR (25 °C, C$_6$D$_6$): δ 135.3 (d with Pt satellites, J_{P-P} = 9 Hz, J_{Pt-P} = 2298 Hz), 128.3 (d, with Pt satellites, J_{P-P} = 9 Hz, J_{Pt-P} = 2284 Hz).

[(C$_5$H$_{10}$N)$_2$PCH$_2$CH$_2$P(NC$_5$H$_{10}$)$_2$]Pt(C$_6$H$_{11}$)H. A solution of [(C$_5$H$_{10}$N)$_2$PCH$_2$CH$_2$P(NC$_5$H$_{10}$)$_2$]Pt(*neo*-Pe)H (**13**) in cyclohexane in a sealed tube was gradually warmed to 45 °C. This afforded [(C$_5$H$_{10}$N)$_2$PCH$_2$CH$_2$P(NC$_5$H$_{10}$)$_2$]Pt(C$_6$H$_{11}$)H in 39% yield. ^{31}P NMR (50 °C, C$_6$H$_{12}$): δ 139.9 (d with Pt satellites, J_{P-P} = 15 Hz, J_{Pt-P} = 1949 Hz), 132.9 (d with Pt satellites, J_{P-P} = 15 Hz, J_{Pt-P} = 2379 Hz).

[(C$_5$H$_{10}$N)$_2$PCH$_2$CH$_2$P(NC$_5$H$_{10}$)$_2$]Pt(CH$_2$SiMe$_2$)H. A saturated solution of [(C$_5$H$_{10}$N)$_2$PCH$_2$CH$_2$P(NC$_5$H$_{10}$)$_2$]Pt(*neo*-Pe)H (**13**) in 1.0 M TMS in cyclohexane was degassed via three freeze–pump–thaw cycles and sealed in an NMR tube. The tube was gradually warmed to 50 °C. This produced [(C$_5$H$_{10}$N)$_2$PCH$_2$CH$_2$P(NC$_5$H$_{10}$)$_2$]Pt(CH$_2$SiMe$_2$)H in quantitative yield. ^{31}P NMR (20 °C, C$_6$H$_{12}$): δ 138.1 (d with Pt satellites, J_{P-P} = 10 Hz, J_{Pt-P} = 2560 Hz), 130.9 (d with Pt satellites, J_{P-P} = 10 Hz, J_{Pt-P} = 2321 Hz).

{[(C$_5$H$_{10}$N)$_2$PCH$_2$CH$_2$P(NC$_5$H$_{10}$)$_2$]Pt}$_2$. When it stood in several solvents, complex **13** exhibited signals assigned to this dimer. ^{31}P NMR (25 °C, cyclohexane): δ 163 (J_{Pt-P} = 449, 2947 Hz).

[(morph)$_2$PCH$_2$CH$_2$P(morph)$_2$]Pt(*neo*-Pe)H (14). A procedure analogous to that given above for [(CyO)$_2$PCH$_2$CH$_2$P(OCy)$_2$]Pt(*neo*-Pe)H (**12**), in which **8** was treated with Na[HB(OMe)$_3$] in THF, was followed. ^{31}P NMR (25 °C, THF): δ 140.5, (d with Pt satellites, J_{P-P} = 13 Hz, J_{Pt-P} = 2315 Hz), 131.6 (d with Pt satellites, J_{P-P} = 13 Hz, J_{Pt-P} = 2366 Hz). ^1H NMR (THF-d_8): δ 3.37 (s, 16 H), 3.36 (m, 16 H), 2.17 (t, 2H, with Pt satellites, J_{Pt-H} = 646 Hz, J_{P-H} = 16 Hz), 1.22 (s, 9 H), 0.32 (s, 4H), –1.07 (d, 1H with Pt satellites, J_{P1-H} = 226 Hz, J_{P2-H} = 12 Hz, J_{Pt-H} = 1148 Hz), –1.52 (d, 1H, with Pt satellites, J_{P1-H} = 226 Hz, J_{P2-H} = 12 Hz, J_{Pt-H} = 1148 Hz).

[(morph)$_2$PCH$_2$CH$_2$P(morph)$_2$]Pt(C$_6$D$_5$)D. Neopentyl hydride **14** was dissolved in C$_6$D$_6$. This solution was transferred to an NMR tube, degassed by means of three freeze–pump–thaw cycles. The tube was sealed and this product was obtained in 83% yield after heating at 40 °C for 6 h. ^{31}P NMR (25 °C, C$_6$D$_6$): δ 133.9 (d with Pt satellites, J_{P-P} = 10 Hz, J_{Pt-P} = 2299 Hz), 125.2 (t of d, with Pt satellites, J_{P-P} = 10 Hz, J_{P-D} = 35 Hz, J_{Pt-P} = 2288 Hz).

{[(morph)$_2$PCH$_2$CH$_2$P(morph)$_2$]Pt}$_2$. After standing in solution in THF for several hours, complex **14** exhibited signals assigned to this dimer. ^{31}P NMR (25 °C, cyclohexane): δ 159.0 (J_{Pt-P} = 58.6, 491, 2885), J_{Pt-Pt} = 3332 Hz).

[–(CH$_2$)$_4$–C(CH$_2$O)$_2$]PCH$_2$CH$_2$P[(OCH$_2$)$_2$C–(CH$_2$)$_4$–]Pt(*neo*-Pe)H (15). A solution of [–(CH$_2$)$_4$–C(CH$_2$O)$_2$]PCH$_2$CH$_2$P[(OCH$_2$)$_2$C–(CH$_2$)$_4$–]Pt(*neo*-Pe)Cl (**10**; 417.9 mg, 0.713 mmol) in 50 mL of THF was treated dropwise with Na[HB(OMe)$_3$] (273 mg, 2.14 mmol) in 15 mL of THF. There was an immediate reaction, causing a yellowing of the solution on addition of the first drops. The solution was cooled in an ice bath for the remainder of the addition, performed dropwise via a Pasteur pipet. A few minutes after the addition was complete, gas evolution occurred, cloudiness developed, and the solution turned orange. After 3 h the solution was warmed to room temperature and the solvent was removed. The residue was extracted with ether, the ether solution was filtered through a frit, and the solvent was removed *in vacuo* (310 mg, 79%). ^{31}P NMR (THF, 20 °C): δ 197.9 (d with Pt satellites, J_{P-P} = 29 Hz, J_{Pt-P} = 2377 Hz), 177.6 (d with Pt satellites, J_{P-P} = 29 Hz, J_{Pt-P} = 2811 Hz). ^1H NMR (THF-d_8, 20 °C): –0.28 (d, 1H, with Pt satellites, J_{P1-H} = 272 Hz, J_{P2-H} = 19.5 Hz, J_{Pt-H} = 1196 Hz), 0.14 (s, 4H), 1.03 (s, 9H), 2.09 (m, 2H, Pt satellites unresolved), 1.2–1.9 (m, 2H).

{[–(CH$_2$)$_4$–C(CH$_2$O)$_2$]PCH$_2$CH$_2$P[(OCH$_2$)$_2$C–(CH$_2$)$_4$–]Pt}$_2$ (17). Freshly prepared neopentyl hydride **15** dissolved in THF was immediately inserted into the NMR spectrometer, and signals assigned to this dimer were detected. ^{31}P NMR (25 °C, THF): δ 239.7 (J_{Pt-P} = 298, 3208 Hz).

[–(CH$_2$)$_4$–C(CH$_2$O)$_2$]PCH$_2$CH$_2$P[(OCH$_2$)$_2$C–(CH$_2$)$_4$–]Pt(THF). The previously described sample exhibited signals assigned to this THF adduct for a few minutes. ^{31}P NMR (25 °C, THF): δ 193.8 (s, J_{Pt-P} = 4537 Hz).

[–(CH$_2$)$_4$–C(CH$_2$O)$_2$]PCH$_2$CH$_2$P[(OCH$_2$)$_2$C–(CH$_2$)$_4$–]Pt(PhC≡CPh) (18). Addition of diphenylacetylene to a solution of the dimer {[–(CH$_2$)$_4$–C(CH$_2$O)$_2$]PCH$_2$CH$_2$P[(OCH$_2$)$_2$C–(CH$_2$)$_4$–]Pt}$_2$ in THF led to the exclusive formation of this diphenylacetylene adduct. ^{31}P NMR (25 °C, THF): δ 181.3 (s with Pt satellites, J_{Pt-P} = 4563 Hz). ^1H NMR (C$_6$D$_6$, 20 °C): δ 7.5 (d), 6.9 (d), 6.5 (s), 3.2 (s), 2.7 (s), 0.27 (s). IR (film on NaCl, cm^{-1}): 3416 (s), 2945 (s), 2825 (s), 1946 (vw), 1883 (vw), 1658 (C=C stretch), 1630 (C=C stretch), 1602, 1496, 1447, 1412, 1370 (s), 1194, 1104 (vs), 1003 (vs), 962 (vs), 786 (vw), 758 (s), 730 (vw), 688 (s), 540 (w), 512 (vw).

[–(CH$_2$)$_4$–C(CH$_2$O)$_2$]PCH$_2$CH$_2$P[(OCH$_2$)$_2$C–(CH$_2$)$_4$–]Pt(MeC≡CMe) (19). Addition of diphenylacetylene to a solution of the dimer {[–(CH$_2$)$_4$–C(CH$_2$O)$_2$]PCH$_2$CH$_2$P[C(CH$_2$O)$_2$–(CH$_2$)$_4$–]Pt}$_2$ in THF led to the exclusive formation of the monomeric adduct **18**. ^{31}P NMR (25 °C, THF): δ 200.13 (s with Pt satellites, J_{Pt-P} = 4229.8 Hz). ^1H NMR (C$_6$D$_6$, 20 °C): δ 3.56 (m, 16 H), 1.402 (m, 12 H), 1.36 (t, H$_3$CCH$_3$, J_{P-H} = 8.48 Hz, J_{Pt-H} = 229.5 Hz). IR (film on NaCl, cm^{-1}): 1644 (C=C stretch).

$[-(CH_2)_4-C(CH_2O)_2]PCH_2CH_2P[(OCH_2)_2C-(CH_2)_4-]Pt(PPh_3)_2$ (20). Addition of PPh_3 to a solution of the dimer in THF produced the bis(triphenylphosphine) adduct in quantitative yield. ^{31}P NMR (25 °C, THF): δ 19.93 (t with Pt satellites, J_{P-P} = 56 Hz, J_{Pt-P} = 3715 Hz), 175.9 (t with Pt satellites, J_{P-P} = 56 Hz, J_{Pt-P} = 5043 Hz). ^1H NMR (C_6D_6, 20 °C): δ7.4 (s), 7.0 (s), 7.6–7.8 (m), 3.5 (s), 3.1 (s), 1.4 (s), 0.29 (s).

$(Cy_2PCH_2CH_2CH_2PCy_2)Pt(neo\text{-}Pe)Cl$. This complex was prepared by an analogous method, using (COD)Pt(*neo*-Pe)Cl and $Cy_2PCH_2CH_2CH_2PCy_2$. ^{31}P NMR (THF 20 °C): δ 10.49 (d with Pt satellites, J_{P-P} = 20 Hz, J_{Pt-P} = 4203 Hz), 6.71 (d with Pt satellites, J_{P-P} = 20 Hz, J_{Pt-P} = 1581 Hz).

$(Cy_2PCH_2CH_2CH_2PCy_2)Pt(neo\text{-}Pe)H$. Treatment of a solution of the neopentyl chloride in THF with $Na[HB(OMe)_3]$ for several hours led smoothly to this neopentyl hydride. ^{31}P NMR (THF, 20 °C): δ 18.6 (d with Pt satellites, J_{P-P} = 19 Hz, J_{Pt-P} = 1732 Hz), 8.2 (d with Pt satellites, J_{P-P} = 20 Hz, J_{Pt-P} = 1871 Hz).

$(Cy_2PCH_2CH_2CH_2PCy_2)Pt(THF)$. In the early stages of the thermolysis of the neopentyl hydride, signals assigned to this THF adduct were detected momentarily at δ 22.8 (s with Pt satellites, J_{Pt-P} = 1906 Hz).

$[(Cy_2PCH_2CH_2CH_2PCy_2)Pt]_2$. ^{31}P NMR spectroscopic analysis of solutions of the neopentyl hydride in cyclohexane revealed signals assignable only to this dimer. ^{31}P NMR (25 °C, cyclohexane): δ 38.7 (J_{Pt-P} = 39.3, 412, 2600 Hz, J_{Pt-Pt} = 3021 Hz).

X-ray Structure Determination of 9. All measurements were made on a Rigaku AFC5R diffractometer with graphite-monochromated Mo Kα radiation and a rotating anode generator.

The structure was solved by direct methods.[43] The non-hydrogen atoms were refined anisotropically. All hydrogen atoms were located in a difference map. The final cycle of full-matrix least-squares refinement[44] was based on 6651 observed reflections ($I > 3.00\sigma(I)$) and 289 variable parameters. Plots of $\sum w(|F_o| - |F_c|)^2$ versus $|F_o|$, reflection order in data collection, $(\sin\theta)/\lambda$, and various classes of indices showed no unusual trends. The maximum and minimum peaks on the final difference Fourier map (excluding two peaks around the platinum atom) corresponded to 0.4 and −0.3 e/Å^3, respectively.

Neutral atom scattering factors were taken from Cromer and Waber.[45] Anomalous dispersion effects were included in F_c;[46] the values for $\Delta f'$ and $\Delta f''$ were those of Cromer.[47] All calculations were performed using the TEXSAN[48] crystallographic software package of Molecular Structure Corp.

Pertinent data collection and reduction information are given in Table 5. The final positional and thermal parameters are included with the supplementary material. Selected bond lengths and angles are presented in Table 4, and an ORTEP drawing is given in Figure 6.

Table 5. Crystal Data and Experimental Details for Structure Determination of 9

formula	$C_{22}H_{41}O_4P_2PtCl_3$
fw	732.96
space group	$P2_1/n$ (No. 14)
a, Å	14.667(3)
b, Å	11.384(6)
c, Å	17.110(4)
β, deg	100.62(2)
V, Å^3	2808(3)
Z	4
d_{calcd}, g/cm^3	1.734
cryst size, mm	0.400 × 0.400 × 0.200
μ(Mo Kα), cm^{-1}	54.74
data collection instrument	Rigaku AFC5R
radiation (monochromated in incident beam)	Mo Kα (λ = 0.710 69 Å)
no. rflns used for unit cell determn; range (2θ), deg	25; 34.7–35.1
temp, °C	−68
scan method	ω–2θ
$2\theta_{max}$, deg	70.2
no. of rflns measd	13 350
no. of unique rflns	12 937 (R_{int} = 0.090)
no. of params refined	289
goodness-of-fit indicator	1.68
correction factors, Lorentz–polarization abs (transmissn factors)	0.59–1.00
R^a	0.048
R_w^b	0.055
largest shift/esd, final cycle	0.00
largest peak, e/Å^3	0.4

$^a R = \sum||F_o| - |F_c||/\sum|F_o|$. $^b R_w = [(\sum w(|F_o| - |F_c|)^2/\sum w(F_o^2)]^{1/2} = 0.055$.

Acknowledgment is made to the donors of the Petroleum Research Fund, administered by the American Chemical Society, for partial support of this research. This work was partially supported by the National Science Foundation (Grant No. CTS-9310198). Additional support was provided by Texaco, Inc. We are indebted to Prof. Martha Teeter, Mr. Akihito Yamano, and Dr. Boguslaw Stec for assistance in solving the X-ray crystal structure. We thank Drs. Mary Faith Hackett, Timothy Miller, and Randall Lee and Prof. George Whitesides for advice and helpful discussions.

Supplementary Material Available: Text and a table giving details of the data collection and structure solution and refinement and tables of positional and thermal parameters, additional bond angles and distances, and general displacement parameters (18 pages). Ordering information is given on any current masthead page.

OM930886Y

(43) Structure solution methods used were as follows. MITHRIL: Gilmore, G. J. *J. Appl. Crystallogr.* **1984**, 42–46. DIRDIF: Beurskens, P. T. DIRDIF: Direct Methods for Difference Structures-an automatic procedure for phase extension and refinement of difference structure factors; Technical Report 1984/1; Crystallography Laboratory, Toernooiveld, 6525 Ed Nijmegen, The Netherlands.

(44) Least-squares: function minimized $\sum w(|F_o| - |F_c|)^2$, where $w = 4F_o^2/s^2(F_o^2)$, $\sigma^2(F_o^2) = [S^2(C + R^2B) + (pF_o^2)^2]/(Lp)^2$, S = scan rate, C = total integrated peak count, R = ratio of scan time to background counting time, B = total background count, Lp = Lorentz–polarization factor, and p = p factor.

(45) Cromer, D. T.; Waber, J. T. *International Tables for X-ray Crystallography*; Kynoch Press: Birmingham, England, 1974; Vol. IV, Table 2.2A.

(46) Ibers, J. A.; Hamilton, W. C. *Acta Crystallogr.* **1964**, *17*, 781.

(47) Reference 45, Table 2.3.1.

(48) TEXSAN-TEXRAY Structure Analysis Package, Molecular Structure Corp., 1985.